BNL-225694-2024-TECH

EIC-ADD-TN-098

Optical Diagnostics with Undulator Radiation for EIC Hadron Ring

I. Pinayev

June 2024

Electron-Ion Collider

Brookhaven National Laboratory

U.S. Department of Energy

USDOE Office of Science (SC), Nuclear Physics (NP)

DISCLAIMER

Optical Diagnostics with Undulator Radiation for EIC Hadron Ring

Igor Pinayev and Gabriele Bassi
Brookhaven National Laboratory

Optical diagnostics is widely used for measurement of the electron beam parameters such as bunch length, beam size, and emittance. Using undulator radiation extends these measurements to the beam energy and energy spread. In this paper, we will study the applicability of synchrotron radiation for protons.

The radiation from a bending magnet is wideband and has substantial divergence in the horizontal plane. The usage of an undulator can substantially increase the brightness of the photon beam. There are three helical undulators available after the CeC experiment [1]. Each of them utilizes permanent magnets and has 62 4-cm periods with a peak field of 1.34 kGs. The vacuum chamber has diamond shape with side size of 28 mm as shown in Fig. 1.

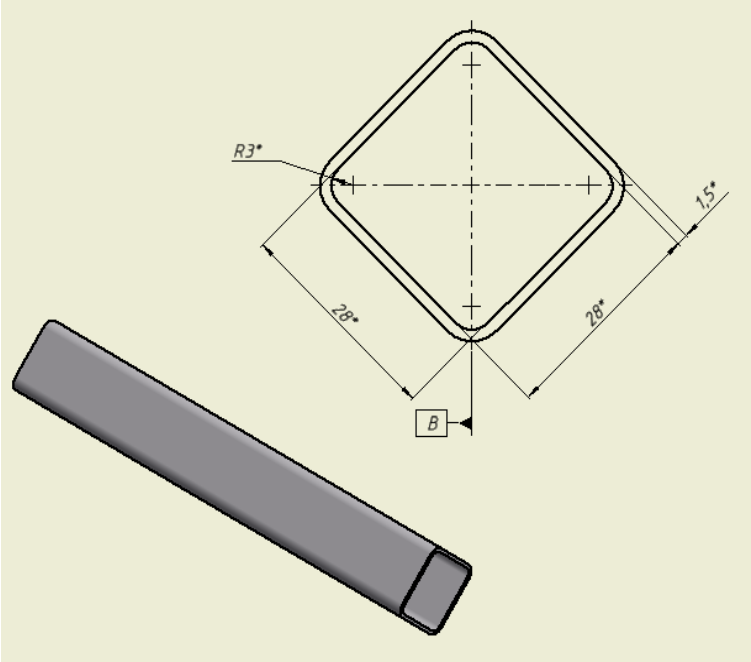

Figure 1: Cross-section of the wiggler vacuum chamber.

This vacuum chamber was already used in the RHIC during regular operations. It was installed in the IR2 region. If needed the gap between the undulator jaws can be increased but the amplitude of the magnetic field will reduce.

Photon flux

A charged particle moving in the oscillating magnetic field emits so-called undulator radiation. The undulator has N periods of length λ_U. The beam with relativistic factor γ will emit radiation at a small angle as shown in Fig. 2.

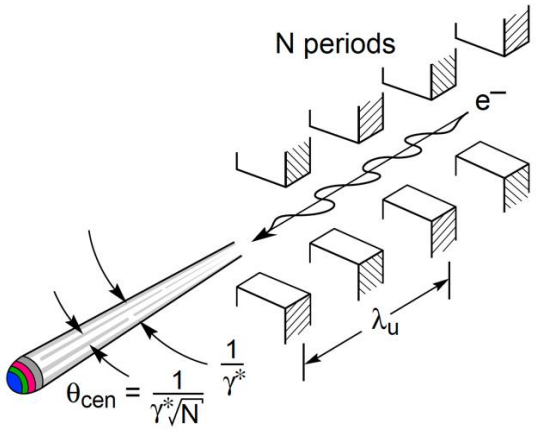

Figure 2: Schematic of undulator radiation.

The radiation wavelength of the planar undulator can be found from the equation below:

$$\lambda_p = \frac{\lambda_U}{2\gamma^2}\left(1 + \frac{K^2}{2} + \gamma^2\theta^2\right) \quad (1)$$

where θ is observation angle, and $K = \frac{eB_U\lambda_U}{2\pi m_0 c}$, where *c* is the speed of light, B_U is undulator peak field, m_0 is particle mass, and *e* is its charge.

For the electrons the deflection parameter *K* can be evaluated from the widely used formula:

$$K = 0.934 B_U[T]\lambda_U[cm] \quad (2)$$

For the protons with larger mass, *K* is:

$$K = 5.085 \times 10^{-4} B_U[T]\lambda_U[cm] \quad (3)$$

and radiated wavelength for practical values of the magnetic field is defined by period, relativistic factor, and observation angle.

The oscillating particles have longer trajectories and their average velocity in the axial direction is less. The effective Lorentz factor γ* can be introduced:

$$\gamma^* = \frac{\gamma}{\sqrt{1+K^2/2}} \quad (4)$$

It also defines the central cone opening angle (where the shift of the wavelength due to the angles equated to the width of the on-axis radiation due to the finite number of periods). The power radiated into the central cone is equal to

$$P_{cen} = \frac{\pi e\gamma^2 I}{\epsilon_0\lambda_U}\frac{K^2}{\left(1+\frac{K^2}{2}\right)^2} \quad (5)$$

where I is circulating current, and ϵ_0 is vacuum permittivity. For the CeC undulators the proton deflection parameter *K* is 2.73x10^{-4}.

The relativistic factor for a 275 GeV proton beam is 293.1 and the corresponding wavelength is 0.233 microns. At 275 GeV 1.0 A circulating beam will emit into the central cone a total power of 9.1 nW or 1.07x10^{10} ph/s.

For the 100 GeV beam (includes gold ions at high energy), the relativistic factor is 106.6 and the wavelength is 1.76 microns. The relativistic factor for gold at injection is 10 and the expected radiation wavelength is 200 microns. Measurement of low-power radiation at this wavelength will be substantially impeded by thermal radiation.

Bunch length measurement

Hamamatsu C16910-01 universal streak camera with S20 cathode covers spectral range from 200 to 850 nm. Time resolution is better than 800 femtoseconds. It can be utilized for bunch length measurements at 275 GeV operation.

For the 100 GeV protons, InGaAs photodiodes can be utilized. Hamamatsu G11193-0.2R has a sensitivity of 0.1 A/W at 1.76 microns wavelength and bandwidths of 1 GHz.

Energy measurement

The undulator deflection parameter is small enough to contribute to the shift of the peak of the spectral power. Propagating radiation through a monochromator and measuring the central wavelength allows us to calculate the relativistic factor $\gamma = \sqrt{\lambda_U/2\lambda}$.

The momentum compaction factor can be evaluated by measurement of the beam energy dependence on the revolution frequency [3].

Beam size measurement

Direct imaging of the beam with reflective optics (protected aluminum MgF2 coating) [2]. The diffraction limit is $\sigma_{diff} = \sqrt{\lambda L_U} = \sqrt{0.23 \times 2.5} = 0.76\ mm$.

Beam divergence measurement

Angular term provides more radiation at longer wavelengths. Asymmetry can be used for divergence calculation. This can be a hard task since angular divergence is small. To alleviate the problem the β-function in undulator can be small. Angular spread in the beam also depends on the energy spread and dispersion value at the location of the undulator. The spectrum modification due to the angular spread were evaluated with MATLAB script using integration over energy spectrum and SRW [4] code as shown in Fig. 3 and Fig. 4.

Asymmetry of the spectrum is more noticeable as shown in Fig. 5, where horizontal emittance was increased 10 times.

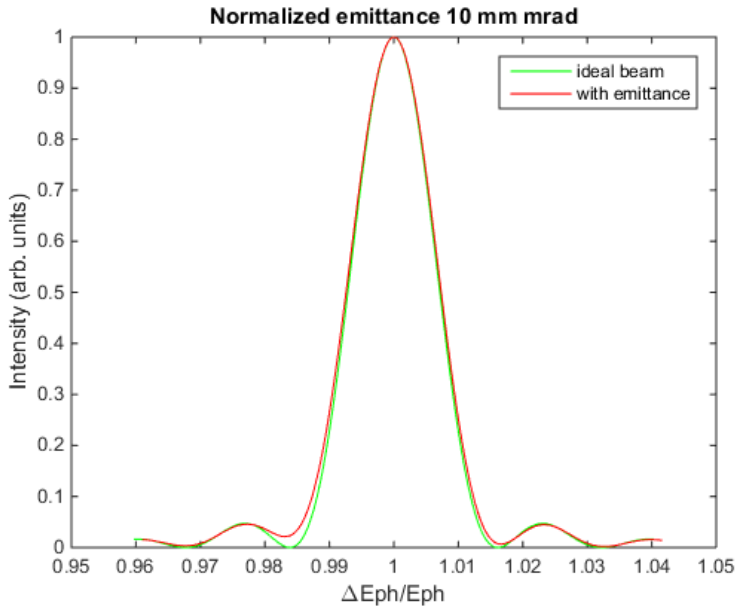

Figure 3: Change of the planar undulator radiation spectrum due to the angular spread caused by emittance (no dispersion). The beam energy is 275 GeV (γ=293.1), and the angular spread corresponds to the β-function of 1 meter. The angular spread causes a redshift of the spectrum (here $\Delta E_{ph}/E_{ph}=1.29\text{x}10^{-3}$) and the red curve is shifted for clarity.

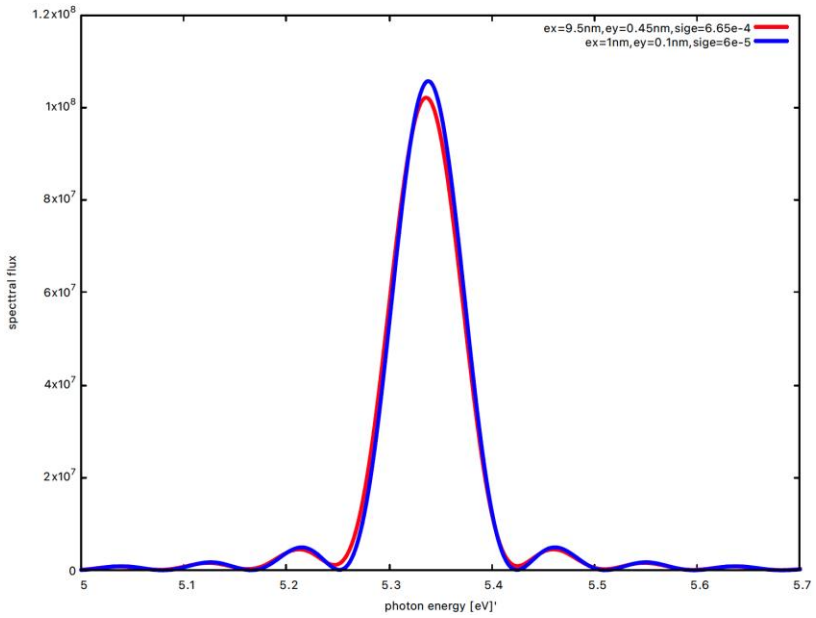

Figure 4: SRW simulation of the helical undulator radiation. The red curve is for the 275 GeV beam with horizontal emittance of 9.5 nm and vertical emittance of 0.45 nm, energy spread is 6.65e-5. The β-functions are equal to 2 meters for both planes. The blue curve is for horizontal emittance and energy spread ten times less, and vertical emittance 5 times smaller. Like with the planar undulator the red shift is observed, and asymmetry of the lower and higher energy tails is also visible.

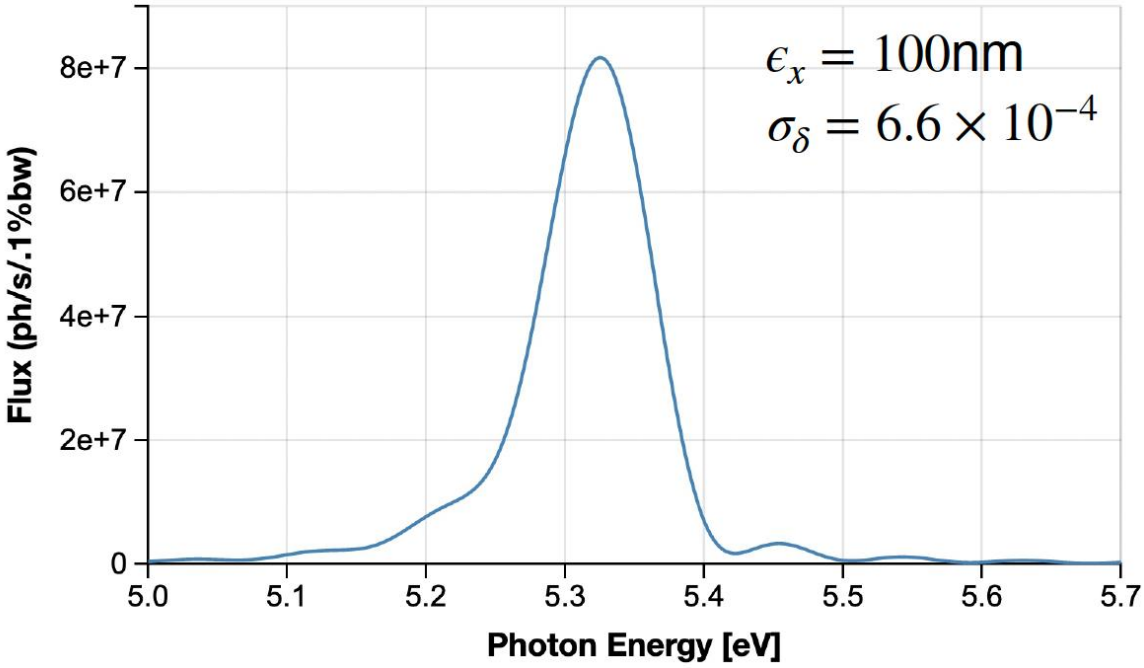

Figure 5: Spectral density of the beam with 100 nm emittance. The asymmetry of the lower energy and higher energy tails is obvious making emittance evaluation straightforward.

Beam energy spread measurement

The particles with different energies emit radiation at different wavelengths. Therefore, the energy spread will cause the widening of the undulator radiation spectrum. Measurement of the spectral width can provide information on the energy spread. Figure 6 shows the SRW simulations for energy spread 10 times larger than nominal value. Now the local minimums in power density are smeared.

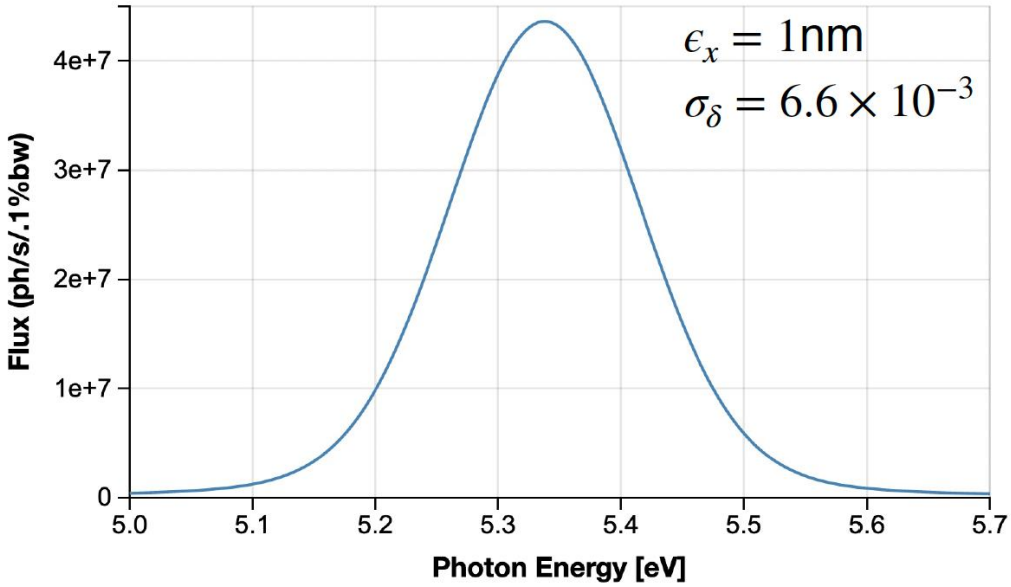

Figure 6: With energy spread of 6.6e-3 the FWHM of the spectrum is doubled.

Real Beam Measurements

With beam having the non-zero emittance and energy spread both factors contribute to the change in the spectrum profile and fit should be utilized to find the energy spread and emittance.

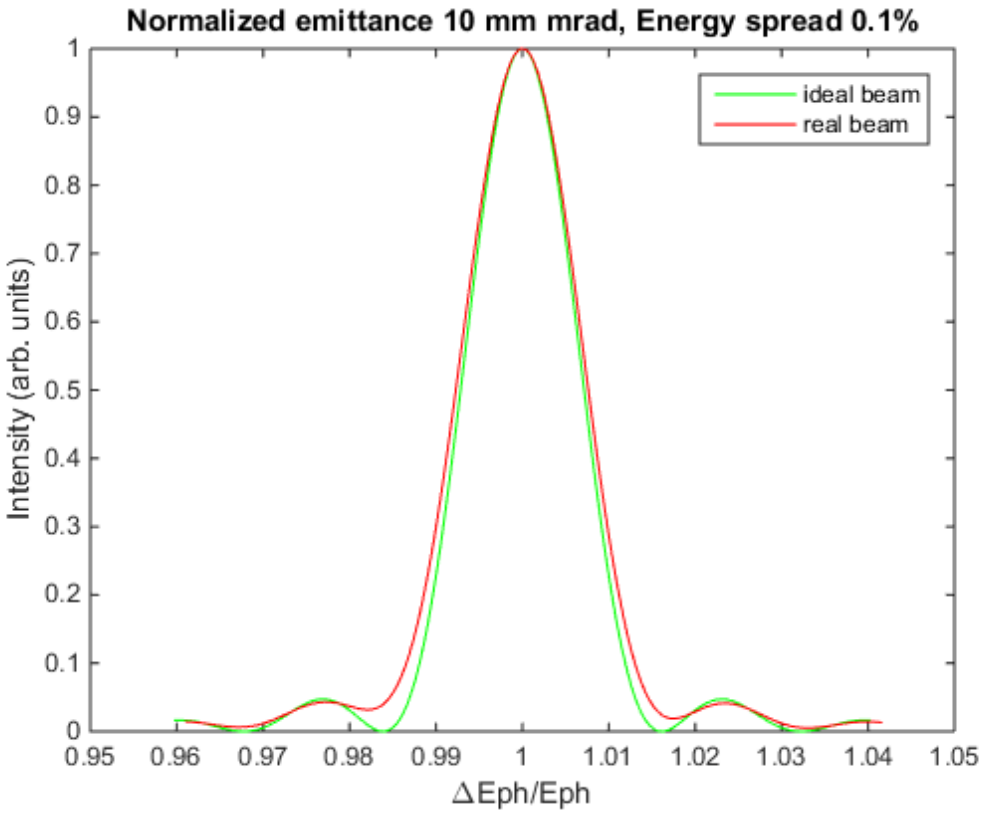

Figure 7: Change of the undulator spectrum due to the energy spread. The change is close symmetric but left minimum is less deep than right one.

References

[1] I. Pinayev et al., "Helical Undulators for Coherent Electron Cooling System", Proc, of FEL'17 Conference, Santa Fe, NM, USA, doi:10.18429/JACoW-FEL2017-WEP051.

[2] B. X. Yang and A. H. Lumpkin, "Simultaneous Measurement of Electron Beam Size and Divergence with an Undulator", Proc. of PAC'99, New York, NY, USA.

[3] B.X. Yang, M. Borland, L. Emory, "High accuracy momentum compaction measurement for the APS storage ring with undulator radiation." AIP Conf. Proc. 546, 234–241 (2000), *https://doi.org/10.1063/1.1342591*

[4] O. Chubar and P. Elleaume, "Accurate and Efficient Computation of Synchrotron Radiation in the Near Field Region", THP01G, in Proc. EPAC'98, pp. 1177-1179.